Molecular Recognition in Poly(ϵ-caprolactone)-Based Thermoplastic Elastomers

Eva Wisse,[†] A. J. H. Spiering,[†] Ellen N. M. van Leeuwen,[†] Raymond A. E. Renken,[†] Patricia Y. W. Dankers,[†] Linda A. Brouwer,[‡] Marja J. A. van Luyn,[‡] Martin C. Harmsen,[‡] Nico A. J. M. Sommerdijk,[†] and E. W. Meijer[†,*]

Laboratory of Macromolecular and Organic Chemistry, Eindhoven University of Technology, P.O. Box 513, NL-5600 MB Eindhoven, The Netherlands, and Department of Pathology and Laboratory Medicine, Medical Biology Section, University Medical Center Groningen, Hanzeplein 1, NL-9713 GZ Groningen, The Netherlands

Received July 14, 2006; Revised Manuscript Received August 15, 2006

The molecular recognition properties of the hydrogen bonding segments in biodegradable thermoplastic elastomers were explored, aiming at the further functionalization of these potentially interesting biomaterials. A poly(ϵ-caprolactone)-based poly(urea) **2** was synthesized and characterized in terms of mechanical properties, processibility and histocompatibility. Comparison of the data with those obtained from the structurally related poly(urethane urea) **1** revealed that the difference in hard segment structure does not significantly affect the potency for application as a biomaterial. Nevertheless, the small differences in hard block composition had a strong effect on the molecular recognition properties of the hydrogen bonding segments. High selectivity was found for poly(urea) **2** in which bisureidobutylene-functionalized azobenzene dye **3** was selectively incorporated while bisureidopentylene-functionalized azobenzene dye **4** was completely released. In contrast, the incorporation of both dyes in poly(urethane urea) **1** led in both cases to their gradual release in time. Thermal analysis of the polymers in combination with variable temperature infrared experiments indicated that the hard blocks in **1** showed a sharp melting point, whereas those in **2** showed a very broad melting trajectory. This suggests a more precise organization of the hydrogen bonding segments in the hard blocks of poly(urea) **2** compared to poly(urethane urea) **1** and explains the results from the molecular recognition experiments. Preliminary results revealed that a bisureidobutylene-functionalized GRGDS peptide showed more supramolecular interaction with the PCL-based poly(urea), containing the bisureidobutylene recognition unit, as compared to HMW PCL, lacking this recognition unit.

Introduction

In soft tissue engineering there is an increasing interest in the functionalization of biomaterials with specific bioactive moieties, such as peptides or growth factors. In general these are introduced either by mixing the bioactive molecules with the desired polymer[1] or via covalent attachment.[2,3] Recently, however, we introduced a modular approach to the functionalization of biomaterials based on supramolecular interactions using different ureidopyrimidinone (UPy)-modified components.[4] This approach involves the simple mixing of a desired bis-Upy prepolymer with selected bioactive molecules functionalized with the same UPy groups to obtain biomaterials tailored toward specific biomedical applications.

Thermoplastic elastomers are promising as biomaterials for cardiovascular tissue engineering since they provide elasticity as well as toughness, which are both required to withstand physiological pressures.[5−7] Biodegradable polyurethane(urea)s based on poly(ϵ-caprolactone) and 1,4-diisocyanatobutane already proved to be biocompatible in vivo and to have the appropriate mechanical properties.[8,9] Moreover, the introduction of biological activity was accomplished by covalent attachment of RGD moieties after surface modification of these polymers.[9]

The objective of our present research program is to use molecular recognition of bisurea moieties[10] to introduce bioactivity in poly(ϵ-caprolactone)-based polyurethane urea via a modular approach. For this we synthesized thermoplastic elastomers **1** and **2** (Chart 1) that both contain poly(ϵ-caprolactone) soft blocks and bisureidobutylene-based hard blocks. These hydrogen bonding segments not only form the reversible cross-links in this polymer, but can also be used to introduce functionalities via specific molecular recognition (Figure 1).[11−13] When compared to polymer **2**, the hard blocks of **1** contain two additional urethane groups per hard block segment. In the present paper we show that this variation in the polymer structure does not significantly affect the mechanical, biomaterial and processing properties. These differences in the hard block segments, however, do have important consequences for the molecular recognition properties of **1** and **2**.

Materials and Methods

General Synthetic Procedures. Benzyl chloroformate, 6-aminohexanoic acid, poly(ϵ-caprolactone)diol (M_n = 1250 and 2000 g/mol), dicyclohexylcarbodiimide (DCC), *p*-toluenesulfonic acid·H_2O, and 4-(*N*,*N*′-dimethyl)aminopyridine (DMAP) were purchased from Acros. Sodium hydroxide (NaOH), 4 Å mol sieves, and Pd/C(10%) were purchased from Merck. Dibutyltin dilaurate, 1,4-diaminobutane, hexylamine, and high molecular weight PCL (80.000 g/mol) were purchased from Aldrich. 1,4-Diisocyanatobutane, sodium dodecyl sulfate (SDS), 1-hydroxybenzotriazole hydrate (HOBt), diisopropylcarbodiimine (DIPCDI), 1,4-diisocyanatobutane, and 6-(Fmoc-amino)caproic acid were purchased from Fluka. Wang-resin (D-1250) loaded with 0.63 mmol

* Corresponding author. E-mail: e.w.meijer@tue.nl.
[†] Eindhoven University of Technology.
[‡] University Medical Center Groningen.

10.1021/bm060688t CCC: $33.50
Published on Web 10/31/2006

Chart 1. Compounds **1**−**5**[a]

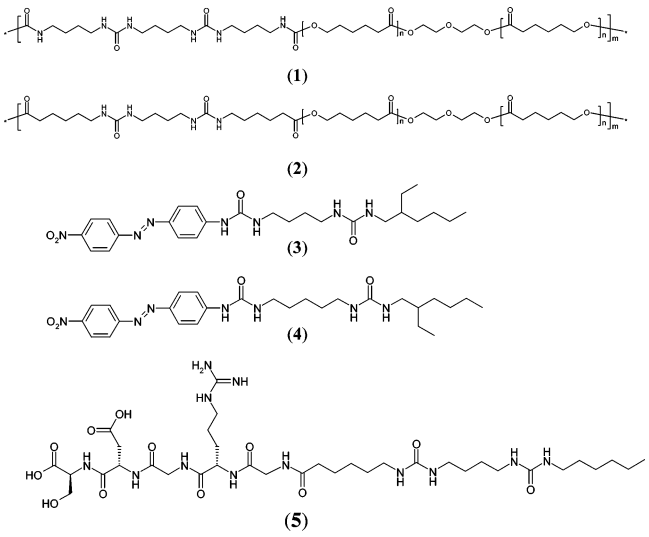

[a] Both Polymers **1** and **2** Were Synthesized with PCL Blocks of M_{2n} = 1250 and 2000.

g^{-1} FMOC-protected serine (FMOC-Ser(tBu)), FMOC-Asp(OtBu), FMOC-Gly, and FMOC-Arg(PMC) were purchased from Bachem (kindly provided by the University of Nijmegen). All solvents were purchased from Biosolve. Deuterated solvents were purchased from Cambridge Isotope Laboratories. Water was always demineralized prior to use. Chloroform was dried over mol sieves. Further chemicals were used without further purification. All reactions were carried out under a dry argon atmosphere, except for the synthesis of peptide **5**. Infrared spectra were measured on a Perkin-Elmer Spectrum One FT-IR spectrometer with a Universal ATR Sampling Accessory. ^{1}H NMR and ^{13}C NMR spectra were recorded on a Varian Gemini (300 MHz for ^{1}H NMR, 75 MHz for ^{13}C NMR) or a Varian Mercury (400 MHz for ^{1}H NMR, 100 MHz for ^{13}C NMR) NMR spectrometer. Molecular weights of the synthesized polymers were determined by GPC using a poly(styrene)-calibrated PL-GPC 120 high-temperature chromatograph that was equipped with a PL gel 5 μm mixed-C column, an autosampler, and an RI detector at 80 °C in 1-methyl-2-pyrrolidinone (NMP). Reversed phase liquid chromatography−mass spectroscopy (RPLC-MS) was performed on a system consisting of the following components: Shimadzu SCL-10A VP system controller with Shimadzu LC-10AD VP liquid chromatography pumps with an Alltima C18 3u (50 mm × 2.1 mm) reversed phase column and gradients of water−acetonitrile−2-propanol (1:1:1 v/v supplemented with 0.1% formic acid), a Shimadzu DGU-14A degasser, a Thermo Finnigan surveyor autosampler, a Thermo Finnigan surveyor PDA detector, and a Finnigan LCQ Deca XP Max.

Synthesis *Poly(urethane urea) **1**_2000.* Polycaprolactonediol (10 g, 5 mmol, M_n = 2000) was dissolved in 100 mL of $CHCl_3$, dried over $MgSO_4$, and filtered during transfer to the reaction flask. Under an argon atmosphere, 1,4-diisocyanatobutane (1.9 mL, 15 mmol) and 4 drops of dibutyltin dilaurate were added to this solution. This solution was refluxed overnight at 85 °C under argon. After precipitation in heptane, a white powder in a yield of 80% was obtained. This isocyanate-functionalized polycaprolactone (9.7 g, 4.2 mmol) was then dissolved in 200 mL of dry $CHCl_3$. Subsequently 1,4-diaminobutane (0.42 mL, 4.2 mmol) was dissolved in 50 mL of dry $CHCl_3$ and slowly added dropwise to the first solution until the isocyanate signal in IR had disappeared. Precipitation in hexane resulted in a white flaky solid in 75% overall yield. FT-IR: ν = 3326, 2943, 2866, 1723, 1680, 1623, 1575, 1538 cm^{-1}. ^{1}H NMR ($CDCl_3$/MeOD): δ = 5.2−5.0 (b, 6H), 4.23 (t, 4H), 4.06 (t, 2(2*n*)H), 3.70 (t, 4H), 3.16 (b, 12H), 2.31 (t, 2(2*n*)H), 1.65 (m, 2(4*n*)H), 1.51 (m, 12H), 1.40 (m, 2(2*n*)H) ppm, with $n \approx 17$. ^{13}C NMR ($CDCl_3$): δ = 173.5, 68.7, 63.9, 63.0, 40.0, 39.7, 33.7, 28.3, 26.9, 26.7, 27.9, 25.1, 24.2 ppm. GPC: M_n= 86 kg/mol, M_w= 192 kg/mol, PD = 2.2.

*Poly(urethane urea) **1**_1250.* This polymer was synthesized in a manner similar to poly(urethane urea) **1**_2000. Overall yield = 56%, FT-IR, ^{1}H NMR ($CDCl_3$/MeOD) and ^{13}C NMR ($CDCl_3$) similar to **1**_2000, with n ≈ 10. M_n, M_w and PD were not determined.

*Poly(urea) **2**_2000.* Poly(ϵ-caprolactone) (M_n = 2000, 10 g, 5 mmol), *N*-carbobenzoxy-6-aminohexanoic acid[14] (2.8 g, 11 mmol), 4-(dimethylamino)pyridinium 4-toluenesulfonate (DPTS)[15] (0.7 g, 2.5 mmol), and DCC (3 g, 15 mmol) were dissolved in $CHCl_3$, and the reaction was allowed to stir for 48 h. The reaction mixture was filtered, and the solvent was evaporated. The remaining solid material was dissolved in 100 mL of $CHCl_3$ and precipitated in hexane. To remove the remaining DPTS, the product was stirred in MeOH. After removing the MeOH, polymer **2a** was obtained as a white powder in a 64% yield (Scheme 1). A solution of **2a** (4 g, 1.6 mmol) in 100 mL of EtOAc/MeOH (v/v 2:1) and 400 mg of 10% Pd supported on activated carbon was subjected to hydrogenation under a H_2 blanket at room temperature for 4 h. After filtration over Celite, the product was isolated by precipitation in hexane, resulting in compound **2b**, as a white powder in a 95% yield. Compound **2b** (14 g, 6.35 mmol) was dissolved in 100 mL of $CHCl_3$. A solution of 560 μL of 1,4-diisocyanatobutane in 5 mL of $CHCl_3$ was slowly added by drops until the signal corresponding to amino methylene protons were no longer visible in ^{1}H NMR. The product was isolated in a 58% overall yield by precipitation in hexane. FT-IR: ν = 3332, 2942, 2866, 1723, 1620, 1575 cm^{-1}. ^{1}H NMR ($CDCl_3$): δ = 5.0−4.8 (b, 4H), 4.23 (t, 4H), 4.07 (t, 2(2*n*)H), 3.70 (t, 4H), 3.18 (b, 8H), 2.31 (t, 2(2*n*+2)H), 1.68 (m, 2(4*n*+2)H), 1.53 (m, 8H), 1.37 (m, 2(2*n*+2)H) ppm, with $n \approx 17$. ^{13}C NMR ($CDCl_3$): δ = 173.5, 158.8, 69.0, 64.1, 63.2, 40.1, 39.8, 34.1, 29.9, 28.3, 27.5, 26.3, 25.5, 24.5 ppm. GPC: M_n = 34 kg/mol, M_w = 102 kg/mol, PD = 3.0.

*Poly(urea) **2**_1250.* This polymer was synthesized in a manner similar to poly(urea) **2**_2000. Overall yield = 31%, FT-IR, ^{1}H NMR ($CDCl_3$/MeOD) and ^{13}C NMR ($CDCl_3$) similar to **2**_2000, with n ≈ 10. GPC: M_n= 56 kg/mol, M_w = 109 kg/mol, PD= 1.9.

*Azobenzene Dyes **3** and **4**:* The synthesis of azobenzene dyes **3** and **4** was reported elswhere.[11]

1-Hexyl-3-(4-isocyanato-butyl)-urea. Diisocyanatobutane (5.5 g, 39.5 mmol) was dissolved in 30 mL of dry chloroform, and a solution of hexylamine (0.4 g, 3.95 mmol) in 10 mL of dry chloroform was added by drops. The reaction was allowed to stir for 30 min after which the reaction mixture was filtered, and the filtrate was reduced in volume and precipitated twice in hexane. A white solid was obtained in quantitative yield. FT-IR: 3325, 2955, 2930, 2860, 2264, 1614, 1571 cm^{-1}. ^{1}H NMR ($CDCl_3$): δ = 4.23 (b, 2H), 3.35 (t, 2H), 3.21 (t, 2H), 3.16 (t, 2H), 1.63, 1.49 and 1.29 (m, 12H), 0.89 (t, 3H).

*(S)-N-((S)-1-Carboxy-2-hydroxy-ethyl)-3-(2-{(S)-5-guanidino-2-[2-(6-{3-[4-(3-hexyl-ureido)-butyl]-ureido}-hexanoylamino)-acetylamino]-pentanoylamino}-acety lamino) succinamic Acid (**5**).* Starting with the Wang-resin loaded with FMOC protected serine (1.5 g, 0.95 mmol), manual peptide chain assembly was carried out using DIPCDI/HOBt-mediated (3.3/3.6 equiv with respect to peptide-resin) couplings in DMF. The Wang-resin loaded with FMOC protected serine was allowed to swell in DMF and the FMOC removal was achieved with 20% piperidine/DMF for 30 min followed by washes with DMF (3 × 5 min). Three equivalents of FMOC-protected amino acids was incorporated in separate syntheses; FMOC-Asp(OtBu) (1.2 g, 2.9 mmol), FMOC-Gly (0.84 g, 2.8 mmol), FMOC-Arg(PMC) (1.9 g, 2.9 mol), and FMOC-Gly (0.84 g, 2.8 mmol) were separately dissolved in DIPCDI/HOBt coupling reagents (6.5 mL) and were allowed to react at least 30 min with the loaded Wang-resin. Kaiser tests, based on ninhydrin, showed the presence of free amine groups after each step, indicating a successful reaction (removal of FMOC or coupling of an amino acid). The obtained product on the resin was washed with dichloromethane (2 × 5 min) and with Et_2O (1 × 5 min) and dried by air. FMOC removal of this FMOC-GRGDS-resin (0.63 g, 0.26 mmol) was achieved with 20% piperidine/DMF, and the GRGDS-resin was washed with DMF (3 × 5 min) and allowed to swell. 6-(Fmoc-amino)-caproic acid (0.32 g, 0.91 mmol) dissolved in 2.1 mL of DMF

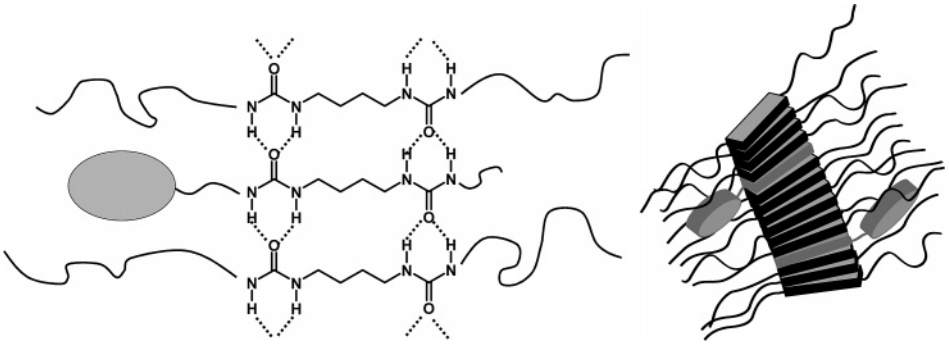

Figure 1. Schematic representation of the desired molecular recognition in the hard segments of the polymers. Grey sphere represents desired functionality.

Scheme 1. Synthetic Route to Polymer **2**

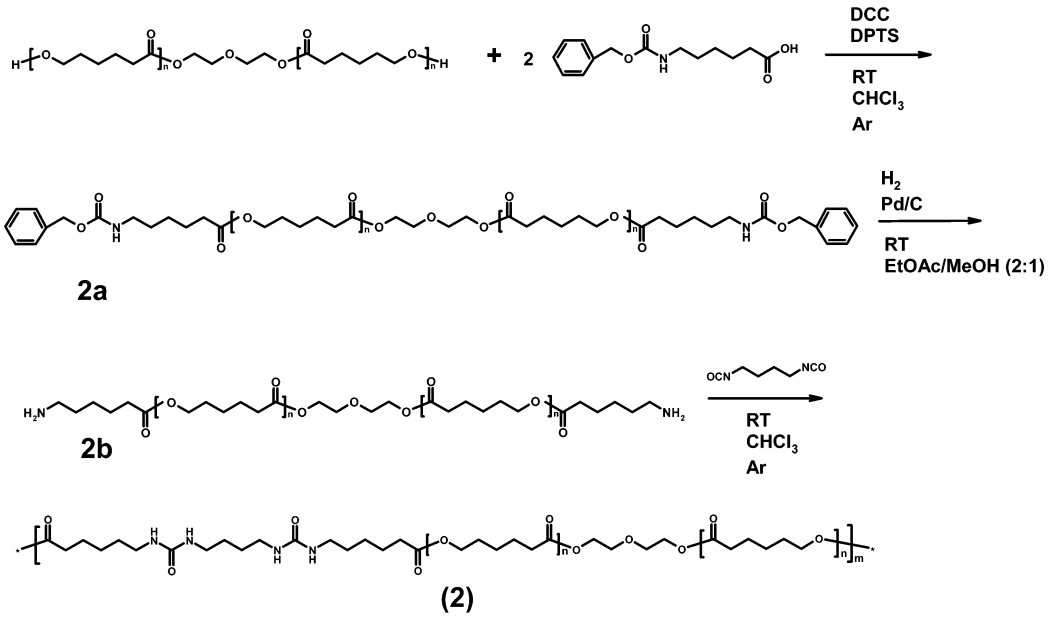

containing DIPCDI/HOBt (1:1:1 equiv) was allowed to react with GRGDS-resin for 1 h and was then washed with DMF (3 × 5 min). FMOC was again removed by 20% piperidine/DMF. Three equivalents of 1-hexyl-3-(4-isocyanato-butyl)-urea (0.10 g, 0.43 mmol), was added and allowed to react overnight. After filtration, the resin was washed three times with DMF and three times with DCM. The product was cleaved off the resin by 95% TFA/H2O (2 mL) at ambient conditions for 6 h, filtered, precipitated in Et_2O and spun down (2 min at 4300 rpm). The product was stirred up in Et_2O and spun down three more times. The white residue was subsequently freeze-dried three times from water with 10−33% acetonitrile, which resulted in a white fluffy powder. No TFA was observed anymore by ^{19}F NMR. RPLC-MS revealed one peak in the chromatogram with *m*/*z* observed mass: $[M + H]^+ = 845.5$ g/mol and $[M + H]^{2+} = 423.3$ g/mol. Calculated mass: 844.96 g/mol.

Azobenzene Dye Release Experiments. Films were cast from solutions containing polymer **1** or **2**, each containing 0.25 w% of either azobenzene dye **3** or **4** (Chart 1). Polymer **1** was cast from $CHCl_3$/MeOH (v/v ∼ 2:1) and polymer **2** from $CHCl_3$. Pieces of the same size were cut from all films and weighed to determine the total amount of dye in each film. The films were placed in 15 mL of a stirred 0.1 M dodecyl sulfate, sodium salt (SDS) solution. UV−vis spectra of the SDS solution were measured on a Perkin-Elmer Lambda EZ210 after different time intervals to determine the amount of dye released. (Extinction coefficient of the dye was found to be 25×10^3 M^{-1} cm^{-1}, $\lambda_{max} = 400$ nm.)

Differential Scanning Calorimetry. Differential scanning calorimetry (DSC) measurements were performed on a Perkin-Elmer Differential Scanning Calorimeter Pyris 1 with Pyris 1 DSC autosampler and Perkin-Elmer CCA7 cooling element under a nitrogen atmosphere. Melting and crystallization temperatures were determined in the second heating run at a heating/cooling rate of 10 °C min^{-1}, glass transition temperatures at a heating rate of 40 °C min^{-1}.

Variable Temperature Infrared. Variable temperature infrared spectra were recorded at an Excalibur FTS 3000 MX from Biorad. All samples were allowed to reach the set temperature for 5 min before recording the IR spectrum.

Optical Microscopy. Flow temperatures were determined using a Jeneval microscope equipped with a Linkam THMS 600 heating device at a heating rate of 2 °C/min.

Atomic Force Microscopy AFM images were recorded at 37 °C in air using a Digital Instrument Multimode Nanoscope IV operating in the tapping regime mode using silicon cantilever tips (PPP-NCH-50, 204−497 kHz, 10−130 N/m). Scanner 6007JVH was used with scan rates between 0.5 and 1 Hz. All images are subjected to a first-order plane-fitting procedure to compensate for sample tilt. Glass cover slips were cleaned by sonicating in acetone, rinsed with acetone, and subsequently dried. AFM samples were prepared by drop casting on the glass cover slips from $CHCl_3$/MeOH (v/v = 9/1) or $CHCl_3$ (1.0 mg/mL) for polymers **1** and **2**, respectively. The solvent was allowed to evaporate under ambient condition and was subsequently dried in a vacuum at 40 °C for approximately 3 h.

Tensile Testing. Tensile bars were punched from polymer films prepared by solution casting polymer films from $CHCl_3$/MeOH (v/v ∼ 8:2) or $CHCl_3$ for polymers **1** and **2**, respectively. After slowly evaporating the solvent, the films were thermally annealed at approximately 20 °C beneath their melting temperatures: 100 °C and 80 °C for polymer **1** and **2**, respectively. Tensile properties were measured

according to ASTM D 1708-96. Grip-to-grip separation in some cases was <22 mm, however, sample rupture at the clamps was never observed. Testing was conducted in a Zwick Z100 Universal Tensile Tester equipped with a 2.5 kN load cell. A crosshead speed of 20 mm/min was used. At least four samples were evaluated for each polymer. Due to the shape of the curves, yield stresses and strains were determined by determining the intersection point of the two tangents to the initial and final parts of the load elongation curves around the yield point.[16] An indicative Young's modulus was determined by calculating the slope at zero strain.

Electrospinning. A homemade electrospinner was used, equipped with a kd Scientific syringe pump and a high voltage source. A 7.4 wt % solution of polymer **1**_1250 in $CHCl_3$/MeOH (v/v = 9:1) was spun at a feed rate of 5−10 μL min^{-1}. The tip-to-target distance was 19 cm and the applied voltage was 15 kV. A 15 wt % solution of polymer **2**_1250 was spun at a feed rate of 15 μL min^{-1}. The tip-to-target distance was 23 cm and the applied voltage was 10 kV.

Cell Proliferation Assay. Films of poly(urea) **2**_2000 were made by drop casting the polymers from THF on glass coverslips (diameter = 1.5 mm). The films were dried in vacuo at 37 °C for at least 2 days and sterilized with UV for at least 2 h. GPC and NMR confirmed that no degradation of the material had occurred during UV treatment. 3T3 mouse fibroblasts were seeded in two densities (1×10^3 cells/cm^2 and 4×10^3 cells/cm^2; medium: 500 mL of DMEM + 500 mL of Ham's F12 + 100 mL of FBS + 5 mL of L-glutamine + P/S) on these films in duplicate in a humidified incubator at 37 °C and 5% CO_2. The cells were studied in time with optical microscopy.

Viability Assay. The cell viability of 3T3 mouse fibroblasts seeded in medium that had been incubated with poly(urea) **2**_2000 was investigated using the LDH (lactate dehydrogenase) leakage kit (Sigma-Aldrich). Drop cast films (from THF) were sterilized with UV for 2 h on each site, prior to use. The polymer was incubated (0.2 g/mL medium) with medium with FBS (composition was the same as described for the cell proliferation assay) for 24 h at 37 °C and 5% CO_2 (no prewash). After that, the medium was refreshed and the polymers (0.2 g/mL medium) were incubated again in medium with FBS for another 24 h at 37 °C and 5% CO_2 (24 h prewash). This procedure was repeated three more times, resulting in samples 48, 72, and 96 h prewash. Latex gloves (negative control; sterilized using the autoclave) and ultrahigh molecular weight polyethylene (positive control; UHMWPE) were used as controls and were treated in the same way, except being incubated twice. The incubated medium (150 μL/well of a 96-well plate) was added to the cells (cultured at a starting density of 2.5×10^3 cells/well in a 96-well plate for 48 h. Beforehand we determined that these cells were 55% confluent at this seeding density after 2 days), and the cells were cultured for 48 h at 37 °C and 5% CO_2.

In Vivo Tissue Reaction. Solution cast films (from THF) of **2**_2000 (diameter = 6 mm, thickness = approximately 0.4 mm) were incubated in demi-water at 37 °C for 3 h, water was then refreshed, and the samples were again incubated overnight. The subsequently dried samples were implanted subcutaneously into male Albino Oxford (AO) rats ($n = 3$ per time point), after sterilization of the disks with UV for at least 2 h on each side. The rats had an age of approximately 10−12 weeks. Animal experiments were carried out according to the NIH guidelines for care and use of laboratory animals. The rats were anesthetized with a mixture of halothane, N_2O, and O_2. The animals were shaved and disinfected. The subcutaneous pockets were made on the back of the rat, three on the right and three on the left side. One sterilized disk was placed in each pocket. The animals were housed in a temperature-controlled (20 °C) and humidity-controlled room with 12 h light/dark cycles after the surgery. They had access to water and standard rat chow adlibitum. Under general inhalation anesthesia, disks were explanted after which the animals were euthanized by cervical dislocation. The disks together with the surrounding tissue were explanted at day 2, 5, 10, 21, and 42 and fixed in glutaraldehyde and embedded in plastic (Technovit 7100 cold curing resin based on hydroxyethyl methacrylate (HEMA), Kulzer Histo-Technik) subsequently. Three disks were implanted for each time point. The tissue slices (thickness = 2 μm) were stained with toluidine blue for histological examination with optical microscopy.

Extraction Experiments. Glass cover slips (1.5 cm ∅) were sonicated in acetone for 15 min, rinsed, and dried by air flow. Polymer **2**_2000 (203.0 mg, 89.45 μmol) was dissolved in 25.0 mL of THF. Functionalized peptide **5** (1.498 mg, 1.773 μmol) was first dissolved in 2.0 mL of THF by sonicating for 10 min, another 3.0 mL of THF was added, and the solution was sonicated for 10 min. Finally 5.0 mL of THF was added, and the solution was sonicated once more. A volume of 12.5 mL of the **2**_2000 solution was added to the solution of **5**. High molecular weight PCL (121.6 mg, 1.52 μmol) was dissolved in 12.50 mL of THF. Peptide **5** (1.559 mg, 1.845 μmol) was dissolved in 1.0 mL of THF by sonicating for 10 min, diluted with 4.0 mL, and again sonicated for 10 min. Finally another 5.0 mL of THF was added. The PCL and peptide **5** solutions were mixed, and 1.0 mL of THF was used to carry over all material. Two polymer films, **2**_2000 with 4 mol % of peptide **5** incorporated (based on the number of bisurea units) and PCL containing the same amount of peptide **5**, were obtained by drop casting 50 μL of the desired polymer solution onto the cleaned microscope glasses. The solvent was allowed to slowly evaporate overnight by covering the samples with a Petri dish. Both films were incubated in 1.00 mL of water at 37 °C for 48 h. The extraction of the peptide out of the polymer films was quantified using reversed phase liquid chromatography−mass spectroscopy (RPLC-MS). Calibration was performed by quantifying one fragment of the parent ion (MS^2) of the peptide, using various concentrations of peptide. The surface area of the corresponding peak in the total ion count was calculated with the ICIS algorithm.

Results and Discussion

Synthesis. Poly(ϵ-caprolactone)diol (PCLdiol) with a M_n of 1250 or 2000 was reacted with a 3-fold excess of 1,4-diisocyanatobutane using dibutyltindilaurate as a catalyst. The resulting macrodiisocyanate was subsequently chain extended with 1,4-diaminobutane to form polyurethane-urea **1** (**1**_1250 and **1**_2000 for polyurethane-ureas containing a PCL block with M_n = 1250 and M_n = 2000, respectively). The synthesis of polyurea **2** (Scheme 1) was less straightforward since functionalizing the PCL prepolymer with amine endgroups leads to intramolecular amidation, resulting in ill-defined, low molecular weight polymers. To circumvent this problem, PCLdiol (M_n =1250, 2000) was reacted with benzyloxycarbonyl-protected α-aminohexanoic acid in a DCC coupling using DPTS as a catalyst. The resulting product was stable in time as was demonstrated by ^{1}H NMR. The subsequent deprotection of the amine was immediately followed by the dropwise addition of 1,4-diisocyanatobutane to obtain maximum chain extension. No amidation was observed, and the characterization of the polymer by ^{1}H NMR, ^{13}C NMR, IR, and GPC confirmed the expected macromolecular structure (**2**_1250 and **2**_2000 for poly(urea) containing a PCL block with M_n = 1250 and M_n = 2000, respectively). The synthesis of azobenzene dyes **3** and **4** was reported elsewhere.[11] The bisurea-functionalized GRGDS peptide was synthesized completely on the solid phase. First GRGDS was synthesized via conventional FMOC-based solid-phase peptide synthesis. Then the free amine of the final amino acid was reacted with 6-(Fmoc-amino)caproic acid as a small spacer between peptide and bisurea functionality. After removal of the FMOC, 1-hexyl-3-(4-isocyanato-butyl)-urea was reacted to the free amine of the spacer to yield the functionalized bisurea-GRGDS peptide **5**.

Morphological, Mechanical, and Biocompatibility Characterization of 1 and 2. For a thermoplastic elastomer to be

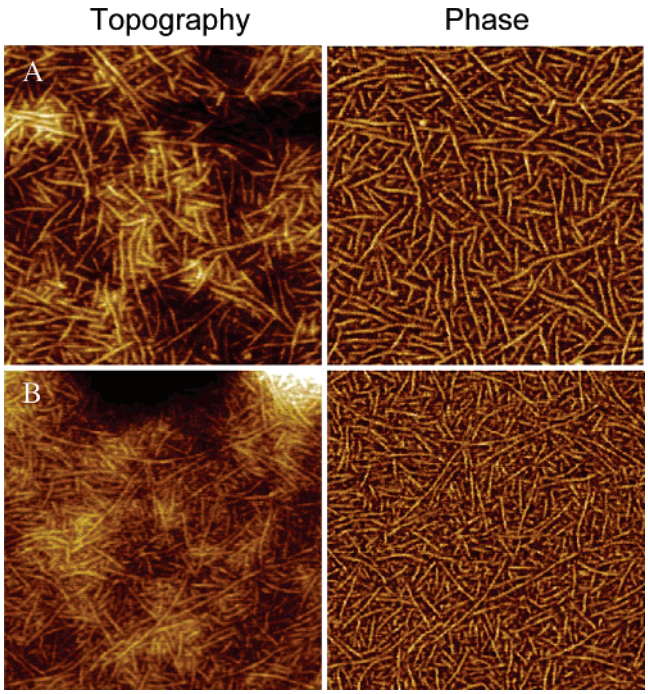

Figure 2. AFM topography and phase images at 500 nm scan sizes of (A) **1**_2000, (B) **2**_2000. Z ranges are 10 nm, $\Delta\phi$ is 15 and 10°, respectively. Data obtained in tapping mode in air at 37 °C. In the phase images the hard phase of the polymer appears brighter than the soft phase.

suitable as a biomaterial for soft tissue engineering, it should be processable into three-dimensional porous scaffolds, mechanically compatible with the tissue of interest, biodegradable, and biocompatible. Therefore the morphological, mechanical, and biocompatibility properties of polymers **1** and **2** are discussed in this paragraph.

Surface Morphology. Polyurethanes and polyurea show well-defined fiberlike morphologies ascribed to the microphase separation of the hard block segments.[17−20] As similar structures were expected for the present polymers, the microphase separation of the hard and soft block domains of both polymer types was studied using AFM in the tapping mode regime. To this end, thin polymer films were deposited on glass by drop casting from chloroform/methanol (v/v = 9/1). After evaporation of the solvent, the films were dried in a vacuum at 40 °C. All measurements were performed at 37 °C to prevent crystalline regions of the soft block from concealing the hard segment morphology. Both types of polymers indeed showed long fibers extending for several hundreds of nanometers which were attributed to stacks of hard blocks embedded in a soft matrix (Figure 2). Although **1** and **2** have distinctly different hard blocks, the apparent width of the observed fibers is 5 ± 1 nanometer for both polymers. Yet, the observed fibers seem to lie closer to each other in the case of polymer **2**. The fact that no significant differences in dimensions could be observed was tentatively attributed to the limited resolution of the AFM tip. The extreme narrow distribution of fiber diameters suggests a cylindrical morphology of the hard segments in both polymer **1** and **2**.

*Processing of Polymers **1** and **2***. Both polymers were processed from solution by electrospinning.[21] Polymer **1**_1250 was spun from a 7.4 wt % solution of methanol/chloroform (9/1, v/v). For polymer **2**_1250 a solution with similar viscosity (as judged by the eye) was obtained at 15 wt % in chloroform. For both polymer solutions, a fine fiber mesh was obtained.

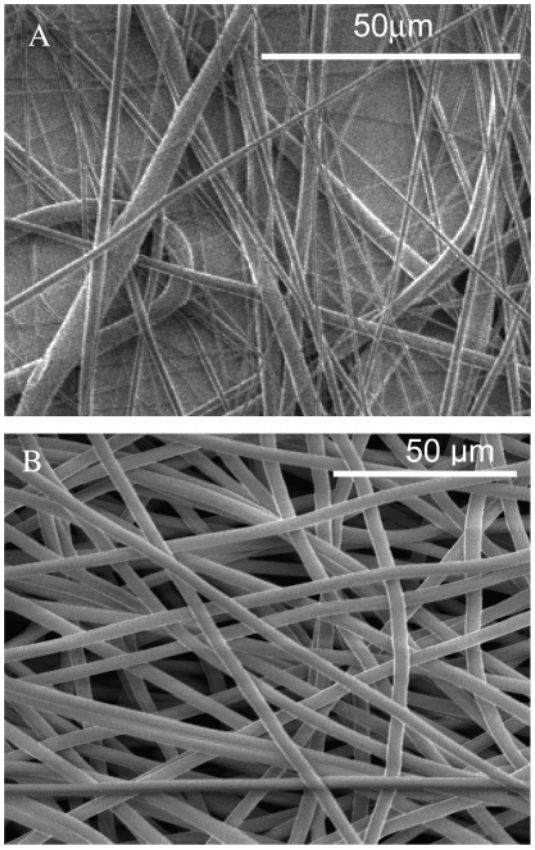

Figure 3. SEM image of fibers of (A) polymer **1**_1250 prepared by electrospinning from 7.4 wt % solution in chloroform/methanol (v/v = 9:1), (B) polymer **2**_1250 prepared by electrospinning from a 15 wt % solution in chloroform.

However, whereas for polymer **2**_1250 fibers with a uniform diameter of 4−5 μm were observed, polymer **1**_1250 yielded a distribution of fiber diameters between 1 and 6 μm (Figure 3). This was attributed to the fact that in the latter case more than one fiber was drawn from the pendant drop at the needle to the ground plate.

*Mechanical Characterization of Polymers **1** and **2***. Mechanical characterization of all polymers was performed by uniaxial tensile testing at room temperature. The mechanical properties directly reflected the different molecular compositions of the polymer (Figure 4 and Table 1). It was found that the Young's moduli of **1**_1250 and **1**_2000 were higher than the moduli of **2**_1250 and **2**_2000, respectively. Polymers **1** were also more brittle compared to their poly(urea) **2** counterparts. This can be attributed to the extra urethane groups in polymer **1**, resulting in a higher hard block to soft block ratio of polymer **1** as compared to polymer **2**.

To be suitable for the intended cardiovascular applications, the scaffolds should have a Young's modulus in the range of a few MPa, purely elastic behavior up to at least 10% strain, and sufficiently high strain at break and tensile strength to prevent in vivo failure.[22,23] The Young's moduli of the four polymers all are between 10 and 40 MPa for bulk samples but will be reduced when these polymers are processed into porous scaffolds. Yield strains were observed between 20 and 30% elongation, which is more than sufficient for the intended applications. Finally, high elongations (700−1500%) and tensile stresses (15−30 MPa) could be reached. Therefore we conclude that the mechanical properties of all four materials are in the right range for cardiovascular tissue engineering scaffold materials.

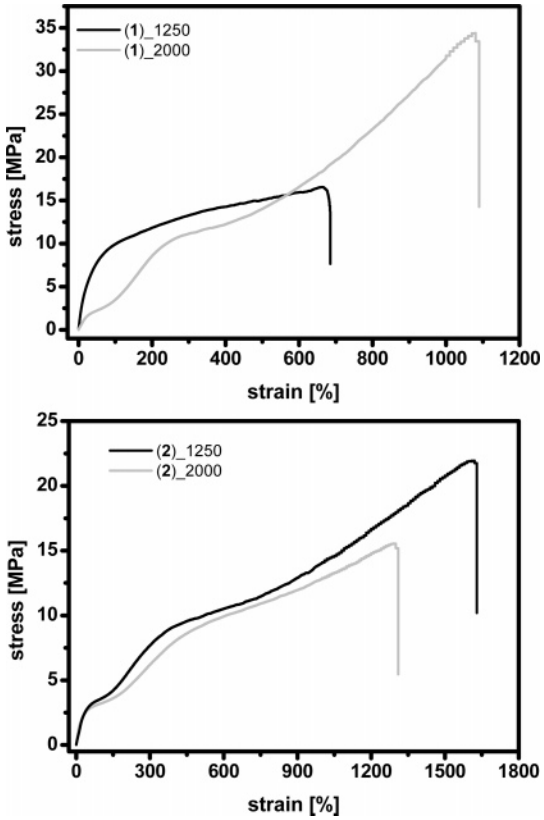

Figure 4. Representative tensile curves (engineering stress) of polymers **1** and **2**, M_n(PCL) = 1250 or 2000.

Table 1. Tensile Properties of Polymers **1** and **2**

polymer_ M_n(PCL)	E [MPa]	σ_{yield} [MPa]	ϵ_{yield} [%]	tensile strength [MPa]	$\epsilon_{at\ break}$ [%]
1_1250	38.7 ± 4.2	8.7 ± 0.4	26.9 ± 0.6	17.8 ± 2.1	700 ± 58
1_2000	16.0 ± 7.9	2.6 ± 1.0	20.2 ± 1.1	30.2 ± 3.8	1114 ± 135
2_1250	11.4 ± 1.0	3.0 ± 0.1	31.8 ± 2.0	21.0 ± 1.5	1505 ± 121
2_2000	13.6 ± 1.6	2.6 ± 0.1	19.0 ± 4.2	15.7 ± 1.6	1330 ± 62.5

Biocompatibility and Biodegradability. Since polyurethane-urea **1** was already shown to be biocompatible,[9] the biocompatibility of only polyurea **2** was studied in vitro and in vivo. In a cell proliferation assay, the proliferation of 3T3 mouse fibroblasts on **2** was compared to cell proliferation on cell culture polystyrene (PS), a known biocompatible material. Cells were seeded at a density of 1×10^3 or 1×10^4 cells/cm^2 in duplicate. Cell proliferation was evaluated by optical microscopy on day 1, 3, 4, and 7 (Figure 5, one sample shown). In all experiments similar behavior was observed for cells seeded on **2** as compared to cells seeded on PS, demonstrating the biocompatibility of poly(urea) **2**.

In a second in vitro biocompatibility test, the cell viability of 3T3 mouse fibroblasts seeded in medium that was incubated with poly(urea) **2**, UHMWPE, or latex was investigated using a LDH (lactate dehydrogenase) test (Figure 6).[24] Every 24 h the medium was refreshed, and all collected medium was used in a LDH activity assay. UHMWPE is known to be biocompatible while latex is not. Cell viability for **2** was only approximately 50% when no prewash was applied. We tentatively attribute this to the presence of small remnants of solvent. All other measurements show high cell viabilities, indicative of a biocompatible poly(urea) **2**.

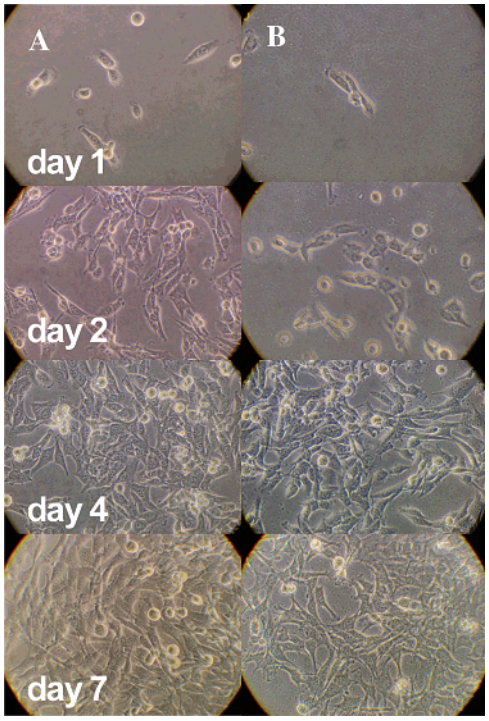

Figure 5. Cell proliferation on PS (A) and **2**_2000 (B) on day 1, 4, 5, and 7, respectively. The cell seeding density was 1×10^3cells/cm^2.

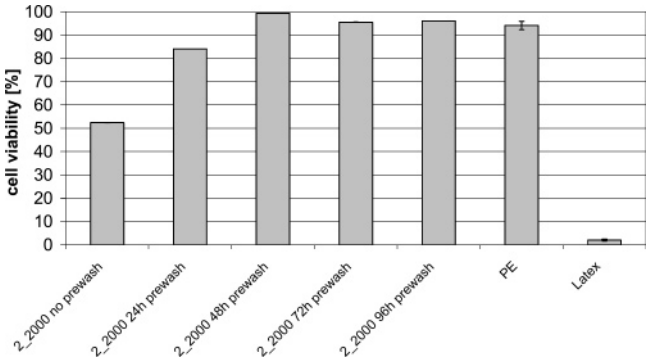

Figure 6. Cell viabilities in medium that had been in contact with poly(urea) **2**, UHMWPE or latex.

Solid disks of polymer **2**_2000 were studied in vivo after subcutaneous implantation in Albino Oxford rats. Explantation was performed after 2, 5, 10, 21, and 42 days (Figure 7). After 2 days, fibrin was present at the interface between the surrounding tissue and biomaterial. Macrophages were infiltrated in the tissue surrounding the implant and vascularization was visible. Only a few lymphocytes and polymorphonuclear cells (PMNs) were observed. On day 5, a layer of fibrin was clearly visible at the interface. The number of macrophages was increased and they were mainly located at the interface. The amount of lymphocytes and newly formed blood vessels was comparable as on day 2. PMNs were not observed anymore. A thin fibrin layer was still present after 10 days. Formation of a few giant cells was observed at the interface and some macrophages infiltrated the biomaterial. These cells showed active phagocytosis of small biomaterial particles. At this point, a thin fibrous capsule has been formed containing elongated fibroblasts. In the surrounding tissue, macrophages were reduced in number and lymphocytes were hardly present. After 21 days, the tissue response became restricted to the interface, whereas the surrounding tissue became quiet. Further signs of slow degradation of the material by a layer of macrophages with

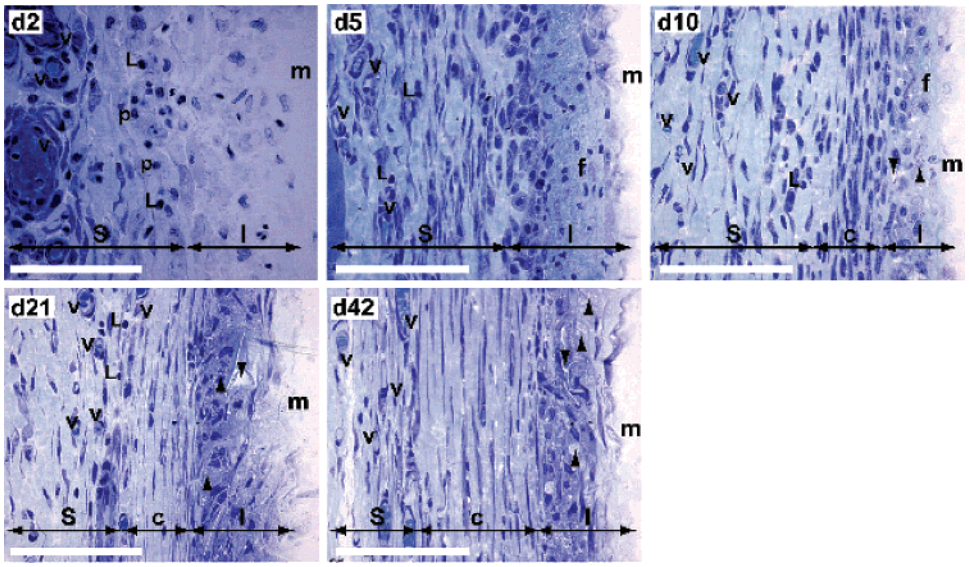

Figure 7. Toluidine blue stained sections of biomaterial **2**_2000 and surrounding tissue on day 2, 5, 10, 21, and 42. The following abbreviations are used: S = surrounding tissue, c = fibrous capsule, I = interface, m = material, L = lymphocyte, P = polymorphonuclear cell, v = blood vessel, f = fibrin, ▲ = macrophage with foamy-like cytoplasm, ▼ = degradation of biomaterial. All scale bars represent 100 μm.

foamy-like cytoplasm were visible at the interface. A mature fibrous capsule has been formed and angiogenesis was slightly increased in the surrounding tissue adjacent to this capsule. After 42 days, phagocytosis by macrophages and giant cells has resulted in a rim of foamy-like cells at the interface, indicating ongoing degradation of the biomaterial.

In conclusion, the in vivo study shows a mild inflammatory response to polymer **2**_2000 characterized by the infiltration of macrophages. Giant cells were formed at the interface. The low numbers of lymphocytes showed that priming of the immune system was hardly involved. Evidence for slow in vivo degradation was found.

Functionalization of Thermoplastic Elastomer (1) and (2) Using Supramolecular Interactions. To investigate the possibility of introducing bisurea-functionalized bioactive molecules into polymers **1** and **2** via molecular recognition, we chose to use bisurea-functionalized azobenzene dyes **3** and **4** as model compounds. The compounds contain a matching bisurea butylene and a nonmatching bisurea pentylene unit, respectively. Polymer films containing dye **3** or **4** were prepared by dissolving both dye and polymer in chloroform/MeOH v/v = 9/1 (**1**_2000) or chloroform (**2**_2000) followed by solution casting. For both polymers the 2000 g/mol PCL variation was chosen, since those two polymers have the best comparable mechanical properties, and, more importantly, both polymers have a semicrystalline PCL soft block at room temperature (see further on: Figures 10 and 11). Equally sized pieces of the films were placed in a stirred 0.1 M sodium dodecyl sulfate (SDS) solution. The release of dye was monitored in time by UV−vis spectroscopy (Figure 8).

In time both compounds **3** and **4** were completely released from the cast films of polymer **1**. However, the release of the matching dye **3** was much slower than the release of nonmatching dye **4**, indicating a higher interaction between polymer **1** and the matching dye compared to the nonmatching dye. When the films were annealed at 20 °C below the melting temperature of the polymer, still 85% of the nonmatching dye **4** was released within 30 h. In contrast, 60% of the matching dye **3** was now retained by the polymer film.

Films of polymer **2** were used after solution casting without thermal annealing, with thermal annealing at 20 °C below the melting temperature of the polymer, or after mechanical loading by stretching the film for 100 times between 0 and 20% elongation at a frequency of 0.5 Hz. Significantly, polymer **2** in all cases was able to retain 70% of the matching dye where

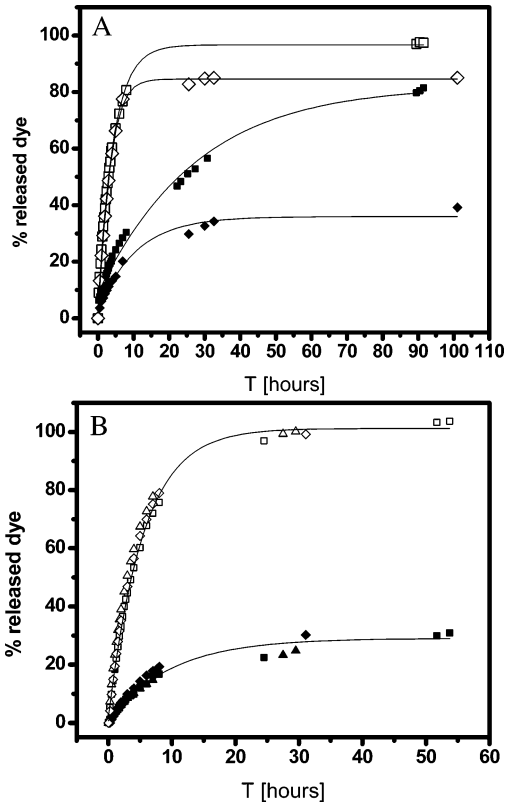

Figure 8. (A) Release profiles of (matching) dye **3** and (nonmatching) dye **4** from films of polymer **1** containing 0.25 wt % of dye. Release curves were measured directly after solvent casting and after thermally annealing the films (4 h at 120 °C). (■ **3** as prepared, □ **4** as prepared, ◆ **3** annealed, ◇ **4** annealed). (B) Release profiles of **3** dye and **4** dye from films of polymer **2** containing 0.25 wt % of dye. Release curves were measured directly after solvent casting, after thermally annealing (4 h at 80 °C) and after mechanical loading of the films (elongating 100 times between 0% and 20% elongation, *f* = 0.5 Hz). (■ **3** as prepared, □ **4** as prepared, ▲ **3** stretched, △ **4** stretched, ◆ **3** annealed, ◇ **4** annealed).

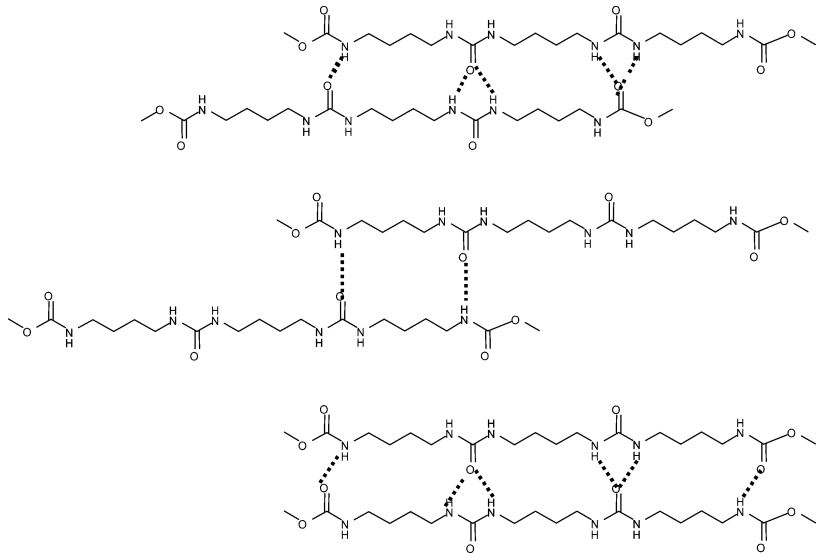

Figure 9. Possible interactions between two hard segments in polymer **1**.

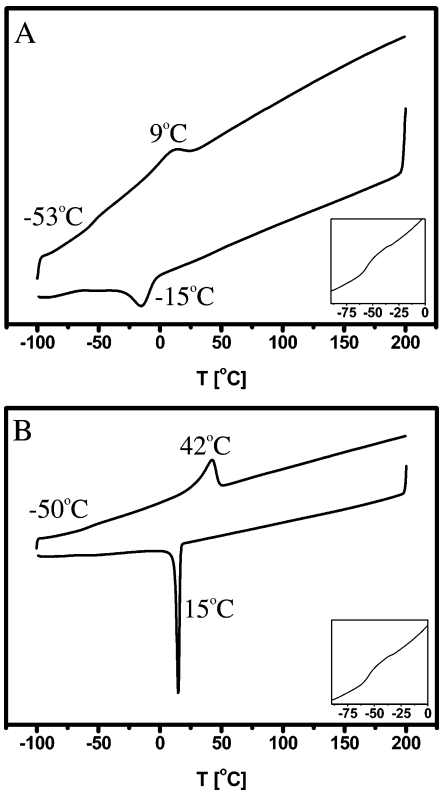

Figure 10. DSC thermograms of (A) **1**_1250 and (B) **1**_2000. Shown curves were recorded at 10 °C/min. Glass transition temperatures were determined from thermograms recorded at 40 °C/min (insets).

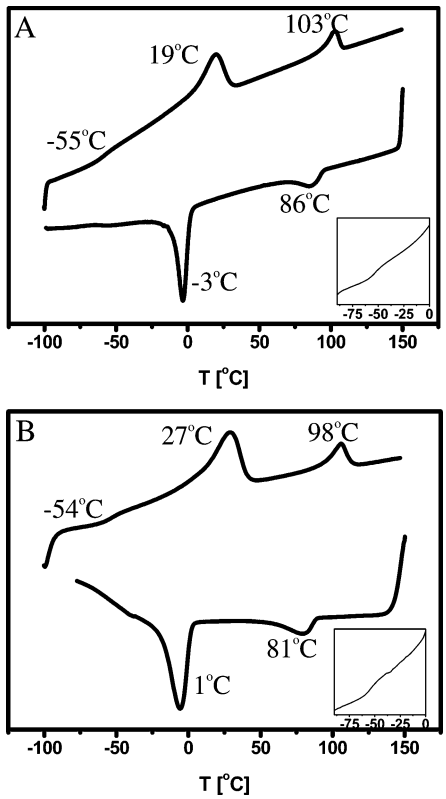

Figure 11. DSC thermograms of (A) **2**_1250 and (B) **2**_2000. Shown curves were recorded at 10 °C/min. Glass transition temperatures were determined from thermograms recorded at 40 °C/min (insets).

as the nonmatching dye was always completely released. This pronounced difference in molecular recognition is surprising as the matching dyes and polymers for both **1** and **2** contain bisureidobutylene moieties. In polymer **1**, however, different additional interactions are possible: urethane groups can hydrogen bond with urea groups and a whole hard block unit can be shifted with respect to the previous hard block in the stack, since urethanes and ureas are also separated by a butylene spacer (Figure 9). Thermal annealing of polymer **1** resulted in an enhanced specificity of the molecular recognition; however, it also led to an enhanced binding of the nonmatching dye **4**.

Thermal Properties of 1 and 2. To further understand the differences in release behavior between polymer **1** and **2**, the thermal behavior of both polymers was studied. Differential scanning calorimetry (DSC) revealed glass transition temperatures of −53 °C and −50 °C for polymer **1**_1250 and **1**_2000, respectively (Figure 10), in both cases close to the glass transition of high molecular weight poly(ϵ-caprolactone) (−60 °C).[25] A single melting peak was observed at 9 °C and 42 °C for polymers **1**_1250 for and **1**_2000 (Figure 10). In the DSC traces of **2**_1250 and **2**_2000 glass transitions were observed at −55 °C **2**_1250 and −54 °C for **2**_2000. In addition, both polymers showed two melting transitions. For polymer **2**_1250 these transitions were observed at 19 °C and 103 °C, whereas those for polymer **2**_2000 were observed at 27 °C and 98 °C (Figure 11).

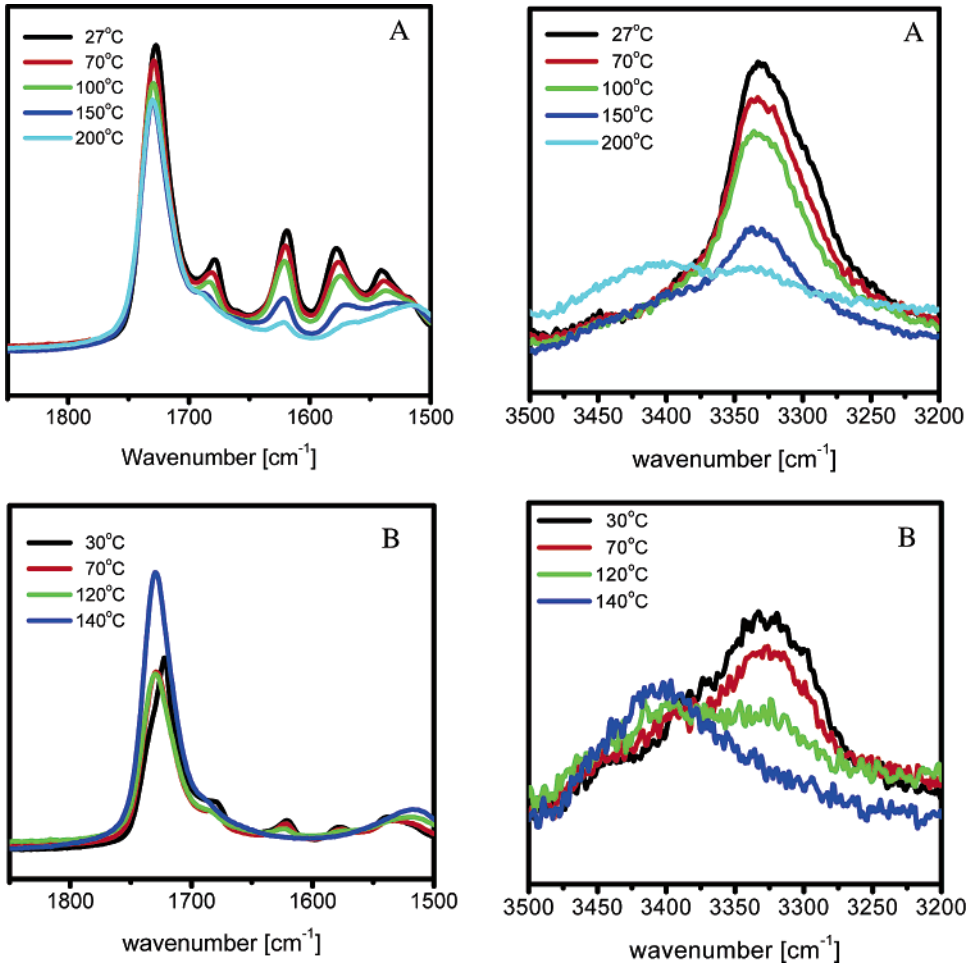

Figure 12. Infrared spectra of (A) **1**_1250, (B) **1**_2000 at increasing temperatures. Characteristic peaks: 1730 cm^{-1}, C═O caprolactone and free C═O urethane; 1690 cm^{-1}, free C═O urea; 1680 cm^{-1}, strongly H-bonded C═O urethane; 1620 cm^{-1}, strongly H-bonded C═O urea; 1575 cm^{-1}, strongly H-bonded amide II; 3330 cm^{-1}, strongly H-bonded N−H; 3400 cm^{-1} free N−H.

To assign these transitions, for all polymers variable temperature IR spectra were recorded at temperatures between 25 and 200 °C (Figures 12 and 13).[26−28] In the IR spectrum of polymer **1**_1250 at room temperature the position of the carbonyl vibrations of the urea (1620 cm^{-1}) and the urethane moieties (1680 cm^{-1}) indicated that both are strongly hydrogen bonded. Upon heating, all peaks decreased in intensity, which was attributed to an increased mobility of the macromolecules and the concomitant reduced dipole moments. At approximately 150 °C the free C═O band of the urea groups started to appear at 1690 cm^{-1}. This, in combination with the reduced intensity of the signal at 1620 cm^{-1}, indicates the breaking of H-bonds related to the melting of the urea hard blocks. However, already at approximately 100 °C we observed the appearance of a vibration at 1685 cm^{-1}, which can either be attributed to a free urea C═O or to a slightly shifted C═O vibration of the H-bonded urethane.

Unfortunately the appearance of the free C═O band of the urethane groups was masked by the overlapping C═O band of the PCL at 1730 cm^{-1}. The free amide II band at 1515 cm^{-1} was rising in intensity from 100 °C onward. Finally, at approximately 140 °C the N−H band started shifting from 3330 to 3400 cm^{-1}. Melting of the bisurea bisurethane hard segments, as evidenced by shifts in the C═O and N−H vibrations, starts at approximately 100 °C; nevertheless, at 200 °C signals corresponding to hydrogen bonded C═O, N−H and amide II groups were still present. From these results we conclude that this polymer shows a gradual melting behavior.

For polymer **1**_2000 similar results were obtained. Both the vibration band of the H-bonded urea carbonyl at 1620 cm^{-1} and the band at 1680 cm^{-1}, corresponding to the band of H-bonded urethane carbonyl groups, had completely disappeared at 140 °C. However, no clear appearance of bands corresponding to the free urea or urethane carbonyl was observed. These peaks are probably obscured by the very broad ester carbonyl band of the PCL segments. Above 70 °C the amide II vibration started shifting to lower wavenumbers; from 1575 to 1515 cm^{-1} at 140 °C. A similar behavior was observed for the NH vibration, shifting from 3330 cm^{-1} toward 3400 cm^{-1}. These data indicate that the melting of the hard segment of polymer **1**_2000 starts around 70 °C and is complete at 140 °C, where hydrogen bonds were no longer observed.

The broad melting transition of the hard segments of both polymers **1** was also observed by optical microscopy. Polymer **1**_1250 first started flowing locally around 125 °C; however, at a heating rate of 2 °C/min it was not until 145 °C before the whole polymer sample was flowing. For polymer **1**_2000 we observed the same behavior, the flow-temperature being 140 °C.

In the IR spectrum of polymer **2**_1250 at room-temperature, vibrational bands were observed corresponding to carbonyl vibrations of PCL, carbonyl vibrations of ureas, and the amide II band at 1730, 1620, and 1575 cm^{-1}, respectively. Up to 106 °C the recorded spectra were still similar to the spectrum at room temperature. However, at 110 °C the aforementioned vibrational bands shifted to 1690, 1540, and 3400 cm^{-1},

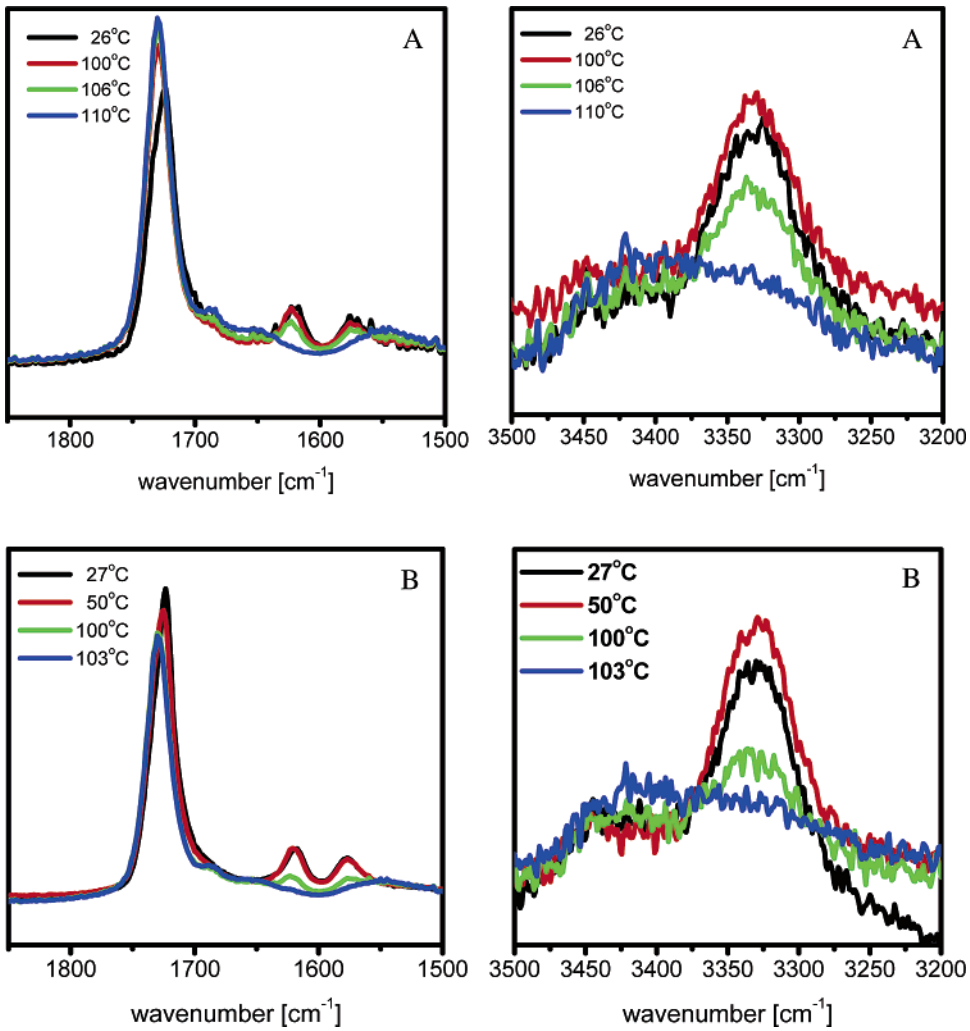

Figure 13. Infrared spectra of (A) **2**_1250, (B) **2**_2000 at increasing temperatures. Characteristic peaks: 1730 cm^{-1}, C═O PCL; 1690 cm^{-1}, free C═O urea; 1650 cm^{-1}, weakly H-bonded C═O urea; 1620 cm^{-1}, strongly H-bonded C═O urea; 1575 cm^{-1} , strongly H-bonded amide II; 3330 cm^{-1}, strongly H-bonded N−H; 3410 cm^{-1}, free N−H.

respectively, indicating the breaking of hydrogen bonds. The sudden flow of **2**_1250 at 112 °C, as observed by optical microscopy, confirmed complete melting of the polymer at this temperature. Nevertheless, there were still some weakly hydrogen bonded urea carbonyls in the melt, as indicated by a small band at 1650 cm^{-1} in the IR spectrum at 110 °C.

Also for polymer **2**_2000, a narrow melting trajectory was observed. At 100 °C the first evidence for some free urea groups was found. At that temperature a band at 1690 cm^{-1} appeared and in addition to the N−H stretch vibration at 3330 cm^{-1} also a significant band appeared at 3410 cm^{-1}. Already at 103 °C the bands at 1620 and 1575 cm^{-1} had completely disappeared, and only vibrational bands corresponding to free groups at 3410, 1690, and 1540 cm^{-1} for the carbonyl, N−H, and amide II bands, respectively, remained. Optical microscopy confirmed again a sudden flow of the polymer at 106 °C.

Biofunctionality via Modular Approach. As a first bioactive functionality, the well-known RGD amino acid sequence, known for its cell-binding properties,[29,30] was functionalized on the solid phase with a bisureidobutylene recognition unit (**5**). We incorporated 4 mol % of peptide **5**, based on the amount of bisurea units, in polymer **2**_2000. The same amount of peptide **5** was mixed with HMW PCL (M_w = 80.000 g/mol). Extraction experiments in water resulted in 26 ± 0.2% of peptide release after 48 h from **2**_2000 and 49 ± 0.02% peptide release from HMW PCL. The significantly higher amount of retained peptide **5** by poly(urea) **2** can be attributed to the molecular recognition between their bisurea units. The observed release of the RGD-peptide could be beneficial for tissue engineering purposes. Initially, sufficient RGD-peptide will be available to facilitate both integrin-mediated adhesion and integrin-mediated survival of cells on the polymer. Upon the continuous release and loss of RGD-peptide from the polymer, adhered cells are prompted to upregulate the secretion of extracellular matrix compounds such as fibronectin and collagens, to further sustain their adhesion and survival. Thus, the transient presence of RGD-peptide may help to adapt the cells to their new substrate.

4. Conclusion

Polymers **1** and **2** are biocompatible and both have mechanical properties that are in the right range for use in soft tissue engineering. Furthermore both polymers are processable from solution, though more reproducible results were obtained for polymer **2**. Clicking bisurea molecules into thermoplastic elastomers using our supramolecular approach is possible when there is a perfect fit between the hydrogen bonding units of the molecules and the polymer. In the case of polymer **1**, we found that matching dye molecule **3** was released much slower than its nonmatching variation **4**. Therefore we concluded that there was a more efficient interaction between the polymer hard blocks and matching dye **3** than with nonmatching dye **4**. The

urethane groups in this polymer are part of the polymer hard block and are separated by a butylene spacer from the urea, the same spacer length as between the two urea groups. Dye **3** can therefore hydrogen bond either to a urethane-butylene-urea or a urea-butylene-urea repeat.

Binding to the urea-butylene-urea repeat in the polymer will result in the strongest interaction between polymer and dye molecule (Figure 9). However, it appears that this is not the dominating interaction, since dye **3** is completely released from the polymer film. When polymer **2** containing a bisureidobutylene hard block was used, a striking difference was observed. Matching dye **3** was released from polymer **2** for only 30% after a few days of washing, while in the same time, nonmatching dye **4** was completely released from the polymer film. The release curves of samples that were prepared by solvent casting without further treatment, thermal annealing after solvent casting or mechanical loading after solvent casting, were exactly overlapping for the matching and nonmatching dyes. Indeed a precise fit between recognition units in both the polymer and the dye molecules results in highly selective incorporation of this dye molecule in the polymer hard block stacks.

The melting behavior of polymers **1** and **2** supports our theory of a perfect fit. For polymer **1** a broad melting transition was observed, while polymer **2** showed a narrow melting trajectory. This behavior is reflecting the organization of the hard blocks in the two polymers. In polymer **1**, hard segments can shift with respect to the next hard segment (Figure 9) resulting in many different type of interactions. Breaking of the different types of interactions appears to happen at different temperatures, resulting in a broad melting transition. In polymer **2** there are only two urea groups involved in hydrogen bonding. In this case, the bisurea segments are stacked exactly on top of each other, causing the narrow melting trajectory.

Both poly(urethane urea) **1** and poly(urea) **2** are in principle suitable as a biomaterial due to their interesting mechanical properties, biocompatibility, and processability. However, bisureidobutylene-functionalized dye molecules can only be incorporated with high selectively into the hard block stacks of poly(urea) **2**. Finally, promising preliminary experiments showed that the bisureidobutylene-containing PCL polymer (**2**_2000) is better capable of retaining the bisurea functionalized GRGDS peptide as compared to the HMW PCL, which might indicate a successful incorporation of bioactivity in the polymer hard block stacks via our proposed modular approach.

Acknowledgment. We acknowledge R. A. A. Bovee and O. L. J. van Asselen for their experimental help and analyses. Financial support from the Neherlands Technology Foundation (STW) and the Dutch Polymer Institute (DPI) are gratefully acknowledged.

References and Notes

(1) Park, H.; Temenoff, J. S.; Holland, T. A.; Tabata, Y.; Mikos, A. G. *Biomaterials* **2005**, *26*, 7095−7103.
(2) Parrish, B.; Breitenkamp, R. B.; Emrick, T. *J. Am. Chem. Soc.* **2005**, *127*, 7404−7410.
(3) Yamaguchi, N.; Kiick, K. L. *Biomacromolecules* **2005**, *6*, 1921−1930.
(4) Dankers, P. Y. W.; Harmsen, M. C.; Brouwer, L. A.; Van Luyn, M. J. A.; Meijer, E. W. *Nature Materials* **2005**, *4*, 568−574.
(5) Fromstein, J. D.; Woodhouse, K. A. *J. Biomater. Sci.-Polym. Ed.* **2002**, *13*, 391−406.
(6) Niklason, L. E.; Gao, J.; Abbott, W. M.; Hirschi, K. K.; Houser, S.; Marini, R.; Langer, R. *Science* **1999**, *284*, 489−493.
(7) Weinberg, C. B.; Bell, E. *Science* **1989**, *231*, 397−400.
(8) Spaans, C. J.; de Groot, J. H.; Dekens, F. G.; Pennings, A. J. *Polym. Bull.* **1998**, *41*, 131−138.
(9) Guan, J. J.; Sacks, M. S.; Beckman, E. J.; Wagner, W. R. *J. Biomed. Mater. Res.* **2002**, *61*, 493−503.
(10) Esch, J. v. S., F.; Loos, M. de; Kooijman, H.; Spek, A. L.; Kellogg, R. M.; Feringa, B. L. *Chem. Eur. J.* **1999**, *5*, 937−950.
(11) Koevoets, R. A.; Versteegen, R. M.; Kooijman, H.; Spek, A. L.; Sijbesma, R. P.; Meijer, E. W. *J. Am. Chem. Soc.* **2005**, *127*, 2999−3003.
(12) Chebotareva, N.; Bomans, P. H. H.; Frederik, P. M.; Sommerdijk, N. A. J. M.; Sijbesma, R. P. *Chem. Commun.* **2005**, *39*, 4967−4969.
(13) Vos, M. R. J.; Jardl, G. E.; Pallas, A. L.; Breurken, M.; van Asselen, O. L. J.; Bomans, P. H. H.; Leclere, P.; Frederik, P. M.; Nolte, R. J. M.; Sommerdijk, N. *J. Am. Chem. Soc.* **2005**, *127*, 16768−16769.
(14) Shah, J. H.; Izenwasser, S.; Geterdouglass, B.; Witkin, J. M.; Newman, A. H. *J. Med. Chem.* **1995**, *38*, 4284−4293.
(15) Moore, J. S.; Stupp, S. I. *Macromolecules* **1990**, *23*, 65−70.
(16) Ward, I. M. S. J. *An introduction to the mechanical properties of solid polymers*; 2nd ed.; John Wiley & Sons: Weinheim, 2004.
(17) Shet, J. P. W., G. L.; Fornof, A. R.; Long, T. E.; Yilgor, I. *Macromolecules* **2005**, *38*, 5681−5685.
(18) Garrett, J. T.; Siedlecki, C. A.; Runt, J. *Macromolecules* **2001**, *34*, 7066−7070.
(19) Pfau, A.; Janke, A.; Heckmann, W. *Surface Interface Anal.* **1999**, *27*, 410−417.
(20) Wu, W.; Huang, J. Y.; Jia, S. J.; Kowalewski, T.; Matyjaszewski, K.; Pakula, T.; Gitsas, A.; Floudas, G. *Langmuir* **2005**, *21*, 9721−9727.
(21) Li, D.; Xia, Y. N. *Adv. Mater.* **2004**, *16*, 1151−1170.
(22) Thubrikar, M. *The aortic valve*; CRS Press: Boca Raton, 1990.
(23) Tai, N. R. M.; Giudiceandrea, A.; Salacinski, H. J.; Seifalian, A. M.; Hamilton, G. *J. Vasc. Surgery* **1999**, *30*, 936−945.
(24) Koh, J. Y.; Choi, D. W. *J. Neurosci. Methods* **1987**, *20* (1), 83−90.
(25) Camacho-Zuniga, C.; Ruiz-Trevino, F. A. *Ind. Eng. Chem. Res.* **2003**, *42*, 1530−1534.
(26) Coleman, M. M.; Skrovanek, D. J.; Hu, J. B.; Painter, P. C. *Macromolecules* **1988**, *21*, 59−65.
(27) Coleman, M. M.; Sobkowiak, M.; Pehlert, G. J.; Painter, P. C.; Iqbal, T. *Macromol. Chem. Phys.* **1997**, *198*, 117−136.
(28) Coleman, M. M.; Lee, K. H.; Skrovanek, D. J.; Painter, P. C. *Macromolecules* **1986**, *19*, 2149−2157.
(29) Pierschbacher, M. D.; Ruoslahti, E. *Nature* **1984**, *309*, 30−33.
(30) Hersel, U.; Dahmen, C.; Kessler, H. *Biomaterials* **2003**, *24*, 4385−4415.

BM060688T